

## ELASTODYNAMIC FIELDS NEAR RUNNING CRACKS BY FINITE ELEMENTS

ZDENĚK P. BAŽANT,† JOHN L. GLAZIK, JR.‡ and JAN D. ACHENBACH§  
Northwestern University, Evanston, IL 60201, U.S.A.

(Received 1 October 1976)

**Abstract**—A finite element method is developed for the computation of elastodynamic stress intensity factors at a rapidly moving crack tip. The method is restricted to bodies whose surfaces and two-material interfaces are either parallel to the direction of propagation or are sufficiently remote. The crack tip starts to move at the instant that it is struck by an incident wave. The finite element grid moves undeformed with the crack tip. The main result consists in the fact that the method of non-singular calibrated crack tip elements, in which the stress-intensity factor is determined from its statically calibrated ratio to the crack opening displacement in an adjacent node, is extended to dynamic problems with moving cracks, for both in-plane and anti-plane motions. The dependence of the calibration ratio on the crack tip velocity is established from previously developed analytical solutions for the near-tip displacement fields. Numerical results compare favorably with known analytical solutions for cracks moving in an infinite solid. The grid motion causes an apparent asymmetric additional damping matrix.

### STATEMENT OF PROBLEM AND OBJECTIVE

There are two principal reasons for significant elastodynamic effects on the fields of stress and deformation near a moving crack tip. They are: rapid application of external loads, and rapid propagation of the crack tip. In both these cases the crack propagates into an environment disturbed by elastic wave motions. It has been shown that stress intensity factors and, therefore, the conditions for further propagation of the crack tip, may be significantly affected by elastodynamic effects. For a recent review of dynamic effects on fracture we refer to [1].

This paper is concerned with the numerical computation of elastodynamic stress intensity factors for a rapidly propagating crack tip, in a field generated by an incident stress wave. The wave strikes the crack tip, and is the cause of crack propagation. Analytical solutions for this kind of problem are available for semi-infinite cracks in an unbounded homogeneous, isotropic, and linearly elastic solid, as discussed in Ref. [1]. For the analysis of more complicated problems, a numerical method appears to be required. Here the effectiveness of the finite element method for elastodynamic problems involving a rapidly propagating crack is explored. The previously formulated method of calibrated crack-tip element [2] is extended to a finite element grid which moves with the crack tip through the elastic solid. The present solution is, however, restricted to bodies whose surfaces and two-material interfaces (if any) are either parallel to the direction of propagation or sufficiently remote (propagation of a crack or cracks along a layer or a layered composite).

For the computation of stress intensity factors, singular elements embodying the correct near tip field have recently been used extensively. For the analysis of wave motions such finite elements have, however, been found rather insufficient [2], and inferior to the "calibrated" crack tip element of ordinary type. For such elements the stress intensity factor,  $K$ , is determined from the

crack opening displacement,  $u_c$ , of the node on the crack surface which is nearest to the crack tip. The value of  $u_c$  usually greatly differs from the correct value, but the ratio  $R = K/u_c$  (calibration ratio) happens to be almost the same for various types of loading, and this ratio can thus be determined in advance by numerical analysis of a simple test case whose exact solution is known. For static problems, this approach has been proposed by Walsh [3]. For elastodynamic problems with stationary cracks, the advantages of a calibrated element over a singular element were demonstrated in Ref. [2]. While for stationary cracks the calibration ratio,  $R$ , is a constant of the grid, for moving cracks it is also a function of the crack velocity  $c$ . It is one purpose of this study to establish the dependence of  $R$  upon  $c$  and to show that the calibrated crack-tip element is also applicable to dynamic problems with rapidly propagating cracks.

### ANTI-PLANE MOTION

Consider a planar crack whose front edge is parallel to axis  $z$ , and which propagates at velocity  $c$  in the direction of axis  $x$  through an isotropic homogeneous elastic solid. Let  $x$ ,  $y$  and  $z$  be cartesian coordinates, (Fig. 1) which move with the crack tip. Attention is first given to the case of anti-plane motion, in which displacements  $u$  and  $v$  in the directions  $x$  and  $y$  vanish. In this case the equation of motion is

$$\frac{\partial^2 w}{\partial x^2} + \frac{\partial^2 w}{\partial y^2} = \frac{1}{c_T^2} \ddot{w} \quad (1)$$

where  $w$  is the displacement in the  $z$ -direction, which depends on  $x$ ,  $y$  and time; and  $c_T = (G/\rho)^{1/2}$  is the velocity of transverse waves,  $G$  being the shear modulus and  $\rho$  the mass density. Superimposed dot denotes the material time derivative. The velocity of a material point is given in the moving coordinates as  $\dot{w} = (\partial w/\partial t) - c(\partial w/\partial x)$  and the acceleration is  $\ddot{w} = (\dot{w})'$ , i.e.

$$\ddot{w} = \left( \frac{\partial}{\partial t} - c \frac{\partial}{\partial x} \right) \left( \frac{\partial w}{\partial t} - c \frac{\partial w}{\partial x} \right). \quad (2)$$

†Professor of Civil Engineering.

‡Graduate Research Assistant.

§Professor of Civil Engineering.

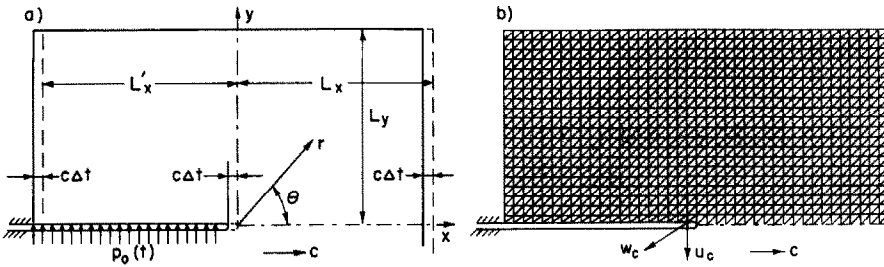


Fig. 1. (a) Coordinate system for the moving crack and (b) the finite element grid used.

### Stress intensity factor

In a sufficiently small neighborhood of the crack tip, the displacement field for any loading is given by the expression (see eqn (4) of Ref. [4]):

$$w(r, \theta, t) = C\sqrt{r}T(t)W(\beta, \theta) \quad (3)$$

in which  $r$  and  $\theta$  are polar coordinates centered at the moving crack tip,  $\theta=0$  being the direction of crack propagation;  $C$  is an arbitrary constant,  $T$  is a function of time  $t$  and  $W$  is a function of angle  $\theta$  and parameter  $\beta = c/c_T$ . The function  $w$  is given by eqns (8, 9, 11 and 12) of Ref. [4]. Evaluating this function for  $\theta = \pi$ , it is found that at the crack surface we have

$$w = CT(t)\sqrt{r}. \quad (4)$$

The stress intensity factor  $K_3$  (for mode III cracks) is defined as

$$K_3 = \lim_{r \rightarrow 0} (\tau_{\theta z} \sqrt{2r}) \quad \text{at } \theta = 0 \quad (5)$$

where  $\tau_{\theta z}$  = shear stress =  $(G/r) \partial w / \partial \theta$ . Substituting eqn (3) for  $w$  and evaluating  $K_3$  in eqn (5) with the help of eqns (8, 9, 11 and 12) from Ref. [4], one obtains

$$K_3 = CT(t)(1 - \beta^2)^{1/2}. \quad (6)$$

A comparison with eqn (4) yields

$$w = K_3 r^{1/2} (1 - \beta^2)^{-1/2} \quad \text{for } \theta = \pi. \quad (7)$$

This holds not only for constant  $c$  but also for smoothly time varying  $c$ .

### Calibrated crack-tip element

It has been shown in a previous study [2] that the singular crack-tip elements, which include the near-tip field given by eqn (3), do not permit accurate and effective numerical solutions in case of wave interaction with cracks. A more effective approach is to use calibrated ordinary-type finite elements near the crack tip. For this approach it is assumed that the ratio of the stress intensity factor to the crack-opening displacement in the nearest node is fixed for all possible loadings and may be determined with the help of a simple test case having a known exact solution.

According to eqn [7], the stress-intensity factor,  $K_3$ , may be calculated from the displacement,  $w_c$ , in the nearest node at the crack surface;

$$K_3 = R w_c, \quad R = C_3 (1 - \beta^2)^{1/2} \quad (8)$$

in which  $R$  is the calibration ratio and  $C_3$  is the constant which should equal  $r_c^{-1/2}$ , according to eqn (7),  $r_c$  being the radial coordinate of the nearest node. In practice, however, the value of  $C_3$  is different because the ordinary finite element near the crack tip does not include the correct near-tip displacement field and because the distance,  $r_c$ , is usually too large for the near tip field in eqn (3) to be accurate.

In the calibrated crack-tip element approach, it is assumed that the value of  $C_3$ , although being grossly different from  $r_c^{-1/2}$  is nearly the same for all possible loadings. For static problems, this has been proposed and demonstrated by Walsh [3]. For dynamic wave problems with stationary cracks, this has been proposed and verified in Ref. [2]. It is one purpose of the present study to demonstrate by numerical results that the coefficient  $C_3$  may be considered to be the same for all velocities of crack propagation. The coefficient  $C_3$  may then be determined from the known solution of a certain static test case, i.e.

$$C_3 = K_3 / w_c \quad \text{for } \beta = 0 \quad (9)$$

$w_c$  being the numerical value obtained from the finite element analysis and  $K_3$  the exact value from the known exact solution for the test case.

### IN-PLANE MOTION

For in-plane motion ( $w = 0$ ), it is convenient to express the displacements  $u$  and  $v$  as

$$u = \frac{\partial \varphi}{\partial x} + \frac{\partial \psi}{\partial y}, \quad v = \frac{\partial \varphi}{\partial y} - \frac{\partial \psi}{\partial x} \quad (10)$$

where  $\varphi$  and  $\psi$  are displacement potentials which satisfy the equations

$$\frac{\partial^2 \varphi}{\partial x^2} + \frac{\partial^2 \varphi}{\partial y^2} = \frac{1}{\kappa^2 c_T^2} \ddot{\varphi}, \quad \frac{\partial^2 \psi}{\partial x^2} + \frac{\partial^2 \psi}{\partial y^2} = \frac{1}{c_T^2} \ddot{\psi}. \quad (11)$$

Here  $\kappa^2 = c_L^2 / c_T^2 = 2(1 - \nu) / (1 - 2\nu)$ ,  $\nu$  being Poisson's ratio, and  $c_L^2$  is the longitudinal wave velocity, which is defined as  $c_L^2 = (\lambda + 2\mu) / \rho$ .

### Stress-intensity factor

In the vicinity of the crack tip we have

$$\varphi(r, \theta, t) = r^{3/2} T(t) \Phi(\alpha, \theta), \quad \psi(r, \theta, t) = r^{3/2} T(t) \Psi(\beta, \theta) \quad (12)$$

where  $\alpha = c / c_L = \beta / \kappa$  and  $\Phi$  and  $\Psi$  are functions defined by eqns (22–24) and (9) of Ref. [4]. Evaluating the

derivatives of these functions at  $\theta = \pi$ , eqn (10) yields

$$v = \frac{3}{2} CT(t)\sqrt{(r)(1-\alpha^2)^{1/2}(1-2/\beta^2)} \quad \text{for } \theta = \pi. \quad (13)$$

The stress intensity factor  $K_1$  (for mode I cracks) is defined as

$$K_1 = \lim_{r \rightarrow 0} (\tau_{\theta\theta} \sqrt{(2r)}) \quad \text{at } \theta = 0 \quad (14)$$

in which  $\tau_{\theta\theta}$  is the circumferential normal stress. If  $\tau_{\theta\theta}$  is expressed in terms of  $u$  and  $v$ , eqns (10) are substituted, and the derivatives of  $\varphi$  and  $\psi$  are calculated at  $\theta = 0$  from eqn (12) in which  $\Phi$  and  $\Psi$  are expressed according to eqns (22-24) and 9 of Ref. [4], then the following relation is obtained

$$K_1 = \frac{3}{4} CT(t) G \kappa^2 \alpha^2 \left[ 1 + \frac{2}{\beta^2} \left( \frac{(1-\beta^2)^{1/2}(1-\alpha^2)^{1/2}}{1-\beta^2/2} - 1 \right) \right]. \quad (15)$$

#### Calibrated crack-tip element

Comparison with eqn (13) yields for the displacement  $v = v_c$  at the location  $r = r_c$  of the nearest node at the crack surface:

$$K_1 = R v_c, \quad R = C_1 \frac{1-2/\beta^2}{2(1-\alpha^2)^{1/2}} \alpha^2 \times \left[ 1 + \frac{2}{\beta^2} \left( \frac{(1-\beta^2)^{1/2}(1-\alpha^2)^{1/2}}{1-\beta^2/2} - 1 \right) \right] \quad (16)$$

where  $C_1 = G \kappa^2 / \sqrt{r_c}$ . However, for the same reasons as explained previously, the value of  $C_1$  in a finite element analysis will be different, and must be calibrated by a test case that may be chosen as the case of a stationary crack, i.e.  $c = \alpha = \beta = 0$ . Calculating the limit of eqn (16) for  $c \rightarrow 0$ ,  $\alpha \rightarrow 0$ ,  $\beta \rightarrow 0$ , one gets

$$C_1 = \frac{K_1}{2(\kappa^{-2} - \kappa^{-4})v_c} \quad \text{for } c = \alpha = \beta = 0 \quad (17)$$

where  $K_1$  is the exact value from the known exact solution of the test case and  $v_c$  is the numerical value obtained by the finite element analysis.

#### FINITE ELEMENT FORMULATION FOR A RAPIDLY MOVING GRID

For the calculation of stress intensity factors by the finite element method, it is convenient to have the finite element grid move through the elastic solid along with the crack tip, at velocity  $c$  in the  $x$ -direction. The region of the grid is taken as a rectangular one in the  $x$ - $y$  plane. Let the surface of the crack be loaded by a distributed load  $p_i$ , and let the opposite side parallel to the crack be subjected to given loads  $p_i$ , or displacements  $u_i$ , and finally, let the boundaries normal to  $x$  be subjected to prescribed displacements. In case that the grid itself is not deforming and the region of the grid is finite, material is flowing into the region of the grid on the side facing the  $x$ -direction and is leaving the region on the opposite side.

The variational equation that is to serve as basis of the

finite element formulation is most easily deduced directly from the differential equation of motion. The equation of motion in moving coordinates reads  $\sigma_{ij,j} - \rho \ddot{u}_i = 0$  where  $u_i$  are the displacement components,  $\sigma_{ij}$  defines the stress tensor, subscripts  $i, j = 1, 2, 3$  refer to cartesian coordinates  $x_1 = x$ ,  $x_2 = y$ ,  $x_3 = z$  moving through the solid and subscripts following a comma denote a derivative. The equations of motion as well as the boundary conditions may be both embodied in the following variational statement

$$\int_V (\sigma_{ij,j} - \rho \ddot{u}_i) \delta u_i \, dV = \int_S (\sigma_{ij} n_j - p_i) \delta u_i \, dS \quad (18)$$

which must hold for any variation  $\delta u_i$  of displacements  $u_i$  which is kinematically admissible. Here,  $u_i$  and  $\delta u_i$  will be restricted to continuous and piece-wise differentiable functions. In eqn (18),  $V$  is the volume of the region moving through the body,  $S$  is the boundary surface and  $n_i$  is its unit outward normal. Expressing the acceleration  $\ddot{u}_i$  similarly to  $\ddot{w}$  in eqn (2), applying the Gauss integral theorem to  $\sigma_{ij,j}$  and noting that  $\sigma_{ij} \delta u_{i,j} = \sigma_{ij} \delta \epsilon_{ij}$ , where  $\epsilon_{ij} = (1/2)(u_{i,j} + u_{j,i}) =$  linearized strain tensor, one obtains

$$\int_V \sigma_{ij} \delta \epsilon_{ij} \, dV + \int_V \rho \left[ \left( \frac{\partial}{\partial t} - c \frac{\partial}{\partial x_1} \right) \left( \frac{\partial u_i}{\partial t} - c \frac{\partial u_i}{\partial x_1} \right) \right] \delta u_i \, dV = \int_S p_i \delta u_i \, dS. \quad (19)$$

This is the variational equation of motion in moving coordinates.

The second integral in eqn (19) involves the term  $c^2 \partial^2 u_i / \partial x_1^2$ . However, for the finite element formulation it is desirable to get rid of the second-order spatial derivatives. To this end, the Gauss theorem may be applied to remove  $\partial^2 u_i / \partial x_1^2$ . This yields

$$\int_V \sigma_{ij} \delta \epsilon_{ij} \, dV + \int_V \rho \frac{\partial^2 u_i}{\partial t^2} \delta u_i \, dV - \int_V \rho c^2 \frac{\partial u_i}{\partial x_1} \frac{\partial (\delta u_i)}{\partial x_1} \, dV - \int_V 2\rho c \frac{\partial^2 u_i}{\partial x_1 \partial t} \delta u_i \, dV = \int_S p_i^* \delta u_i \, dS + \int_V \left( \rho \frac{\partial c}{\partial t} + \rho c \frac{\partial c}{\partial x_1} + c^2 \frac{\partial \rho}{\partial x_1} \right) \frac{\partial u_i}{\partial x_1} \delta u_i \, dV \quad (20)$$

in which

$$p_i^* = p_i + p_i^a; \quad p_i^a = -\rho c^2 \frac{\partial u_i}{\partial x_1} n_i. \quad (21)$$

Here,  $p_i^a$  represents an apparent, additional distributed load that must be applied on the surface of the moving region. This would very much complicate the finite element formulation because load  $p_i^a$  depends on displacements (and does not represent a natural boundary condition associated with some extremum principle). Fortunately, however,  $p_i^a = 0$  on the crack surface because  $n_i = 0$ . On the remaining boundary segments  $p_i^a$  need not be considered because either  $n_i = 0$  or  $\delta u_i = 0$ ; but these boundary conditions are irrelevant (see eqn 28).

Equation (20) is valid even when the velocity of grid points,  $c$ , depends on  $t$  and  $x_1$ . In the present study,

attention will now be restricted to time-constant velocity  $c$  and to a grid which does not deform as it moves through the solid, and also to a medium of uniformly distributed mass. Then the volume integral on the right-hand side of eqn (20) vanishes because  $\partial c/\partial t = \partial c/\partial x_1 = \partial \rho/\partial x_1 = 0$ .

The usual notations are introduced for the finite element formulation, i.e.  $\mathbf{q}$  = column matrix of nodal displacement of the finite element;  $\mathbf{u}$  = column matrix consisting of displacements  $u$ ,  $v$  and  $w$ ;  $\boldsymbol{\sigma}$ ,  $\boldsymbol{\epsilon}$  = column matrices formed of the stress and strain components  $\sigma_{ij}$  and  $\epsilon_{ij}$ . Furthermore  $\mathbf{u} = \mathbf{C}\mathbf{q}$  and  $\boldsymbol{\epsilon} = \mathbf{B}\mathbf{q}$  where  $\mathbf{C}$  and  $\mathbf{B}$  are well known rectangular matrices depending on  $x_i$ , and  $\boldsymbol{\sigma} = \mathbf{E}\boldsymbol{\epsilon}$  where  $\mathbf{E}$  is the matrix of elastic constants. Substitution into the variational relation in eqn (20) yields

$$\sum_{el} \left\{ \int_{el} (\mathbf{B}\delta\mathbf{q})^T \mathbf{E}\mathbf{B}\mathbf{q} dV_{el} + \int_{el} \rho(\mathbf{C}\delta\mathbf{q})^T \mathbf{C} \frac{d^2\mathbf{q}}{dt^2} dV_{el} - \int_{el} \rho c^2 \left( \frac{\partial \mathbf{c}}{\partial x} \delta\mathbf{q} \right)^T \frac{\partial \mathbf{C}}{\partial x} \mathbf{q} dV_{el} - \int_{el} 2c\rho(\mathbf{C}\delta\mathbf{q})^T \frac{\partial \mathbf{C}}{\partial x} \frac{d\mathbf{q}}{dt} dV_{el} \right. \\ \left. = \int_S p_i^* \delta u_i dS \right. \quad (22)$$

in which subscript  $el$  refers to individual finite elements and superscript  $T$  denotes the transpose of the matrix. Equation (22) may be rewritten as

$$\sum_{el} (\delta\mathbf{q})^T \left( \mathbf{M} \frac{d^2\mathbf{q}}{dt^2} + \mathbf{D} \frac{d\mathbf{q}}{dt} + \mathbf{K}\mathbf{q} \right) = \int_S p_i^* \delta u_i dS \quad (23)$$

in which

$$\mathbf{K} = \mathbf{K}_1 + \mathbf{K}_2, \quad \mathbf{K}_2 = - \int_{el} \rho c^2 \frac{\partial \mathbf{C}^T}{\partial x} \frac{\partial \mathbf{C}}{\partial x} dV_{el} \quad (24)$$

$$\mathbf{D} = \mathbf{D}_1 + \mathbf{D}_2, \quad \mathbf{D}_2 = - \int_{el} 2c\rho \mathbf{C}^T \frac{\partial \mathbf{C}}{\partial x} dV_{el} \quad (25)$$

Here  $\mathbf{K}_1$ ,  $\mathbf{D}_1$  and  $\mathbf{M}$  are the usual stiffness, damping and mass matrices for immobile grid ( $c = 0$ ); and  $\mathbf{K}_2$  and  $\mathbf{D}_2$  are apparent additional stiffness and damping matrices, which depend on  $c$ . In the present case  $\mathbf{D}_1 = 0$  because no physical damping is considered. In a wave propagation problem, the mass matrix is properly considered as lumped [2]. However, even when all mass is assumed to be lumped in the nodal points, matrix  $\mathbf{D}_2$  is not diagonal in case of a moving grid.

The presence of the damping matrix is unfavorable to the use of explicit numerical integration of the equations of motion because the term  $\mathbf{D} d\mathbf{q}/dt$  must be considered as given, being evaluated on the basis of  $d\mathbf{q}/dt$ , in the previous time step, which introduces a further error. Another complicating feature brought about by the movement of the coordinate system is the fact that the equation system to be solved at each time step has a non-symmetric matrix, because the apparent damping matrix in eqn (25) is, obviously, non-symmetric. This makes the solution of implicit equations by Gaussian elimination relatively disadvantageous, as compared to Gauss-Seidel iteration. However, the iterative solution is, in case of wave problems, rather efficient, and converges very rapidly because the mass matrix makes the diagonal terms large and because a good initial estimate of the solution is available from the previous time step.

#### NUMERICAL RESULTS FOR WAVE DIFFRACTION BY A MOVING CRACK

Let the crack in Fig. 1 be subjected to a wave with a front parallel to axis  $x$  and  $z$  and arriving at time  $t = 0$  from the positive  $y$ -direction. Assume that the crack begins to propagate at constant velocity  $c$  as soon as the wave arrives at the crack tip ( $t = 0$ ). In view of the superposition principle, the solution consists of two parts; one part represents a wave passing through as if no crack existed, and the other part represents the effect of applying on the surface of the propagating crack a load which cancels the stress at that location from the first part of the solution. Only the second part of the solution needs to be calculated. In particular, consider that a uniform load  $p = p(x, t)$  which is a Heaviside step function of time,  $p(x, t) = p_0 H(t)$ , is applied on the surface of the propagating crack. Load  $p$  is an antiplane shear stress in case of an antiplane shear wave, and a normal stress in case of an incident longitudinal wave. The exact solution to this problem for any  $c$  is known; for antiplane motions, the solution is (p. 44 of Ref. [1]):

$$K_3 = \frac{2}{\pi} p_0 \sqrt{(2c_T t)} \quad \text{for } c = 0 \quad (26)$$

$$K_3 = \frac{2}{\pi} p_0 \left[ 1 - \frac{c}{c_T} \right]^{1/2} \sqrt{(2c_T t)} \quad \text{for } 0 \leq c \leq c_T$$

and for in-plane motions, the solution is (eqn (52) of Ref. [5]).

$$K_1 = \frac{2}{\pi} \frac{p_0 c_1}{F_+(0)} \frac{1 - \epsilon^2/2}{(1 + \epsilon)^{1/2}} (tc_T)^{1/2} \left\{ \frac{(1 - \epsilon^2)^{1/2}}{1 - \epsilon^2/2} - \frac{1 - \epsilon^2/2}{(1 - \alpha^2)^{1/2}} \right\} \quad (27)$$

where

$$\epsilon = c/c_T, \quad \alpha = c/c_L \\ c_1 = \frac{(1 - \alpha^2)^{1/2} (1 - \epsilon^2)^{1/2}}{(1 - \alpha^2)^{1/2} (1 - \epsilon^2)^{1/2} - (1 - \epsilon^2/2)^2} \quad (28)$$

$$F_+(0) = \frac{c_T - c}{c_R - c} \exp \left( \frac{1}{\pi} \int_{(c_L - c)^{-1}}^{(c_T - c)^{-1}} \tan^{-1} \left\{ \frac{\left[ w^2 - \frac{(1 + cw)^2}{2c_T^2} \right]^2}{w^2 \left[ w^2 - \frac{(1 + cw)^2}{c_L^2} \right]^{1/2} \left[ \frac{(1 + cw)^2}{c_T^2} + w^2 \right]^{1/2}} \right\} \frac{dw}{w} \right)$$

A finite element grid, moving with the crack through the solid as a rigid body, is introduced within the rectangular region, as shown in Fig. 1. Since it is impossible to avoid spurious wave reflections at the boundary, the distances,  $L_x$ ,  $L'_x$  and  $L_y$ , from the crack tip to the boundary must be such that the time of travel of a wave from the crack tip to the boundary and back exceeds for all boundary points a specified time  $T_1$  (the longest time for which the solution is sought). In the  $y$ -direction, the wave speed relative to the moving grid is  $c_T$ , and therefore:  $L_y \geq (1/2)c_T T_1$ . However, in the positive  $x$ -direction the relative wave speed is  $c_T - c$ , and in the negative  $x$ -direction it is  $c_T + c$ . This yields for the travel times of the waves reflected from the right and left boundaries the conditions  $T_1 \leq L_x/(c_T - c) + L'_x/(c_T + c)$ , and  $T_1 \leq L'_x/(c_T + c) + L_x/(c_T - c)$ . Solving  $L_x$  and  $L'_x$  from these

two conditions one obtains

$$\text{Min } L_x = \text{Min } L'_x = L_0 \left(1 - \frac{c^2}{c_T^2}\right), \quad \text{Min } L_y = L_0,$$

$$L_0 = \frac{1}{2} c_T T_1. \quad (28)$$

If these conditions are satisfied, then the type of boundary conditions (other than those at the crack surface) is irrelevant for the solution of the stress intensity factor up to the time  $T_1$ . Note that the longitudinal dimension of the region can be taken smaller than the transverse dimension and could be reduced with increasing crack speed. Nevertheless, for convenience of programming,  $L_x = L'_x = L_y = L_0$  was used in all numerical calculations for all crack speeds. It is also interesting, but not surprising, to note that the transformation of length  $L_0$  in this equation corresponds to the Lorentz transformation in the theory of relativity.

A regular grid of equal size finite elements has been introduced, as shown in Fig. 1(b), yielding a nonsymmetric system of 861 equations of bandwidth 44 for the antiplane motion, and 1722 equations of bandwidth 88 for the inplane motion. Triangular constant strain elements have been used because they seem to be best for wave propagation problems with a sharp front [2]. The stress intensity factors have been calculated from the displacement  $w_c$  or  $u_c$  in the nearest node on the crack surface (see Fig. 1(b)). To calibrate the crack-tip element, the program has first been run for the case  $c = 0$  for which the exact solution is given in Ref. [2]. Finite element programs have been written for both the antiplane and the inplane motions. The integration in time has been carried out in time steps, using Anderson's version of the implicit Newmark  $\beta$ -algorithm (with  $\beta = 1/4$ ), as has been described in [2]. The time step,  $\Delta t = h/c_T$  or  $h/c_L$  has been used,  $h$  being the element size. In each time step, the equation system has been solved by Gauss-Seidel iteration, using an overrelaxation factor of 1.15,

which proved to be optimum. Only about 10 iterations have been needed to achieve convergence up to three significant digits.

The numerical results for  $K_3(t)$  and  $K_1(t)$  at various crack propagation velocities  $c$  are plotted in Fig. 2. The dependences of  $K_3$  and  $K_1$  at the final time  $T_1$  from Fig. 2 upon crack velocity  $c$  are plotted in Fig. 3(a, b) and the exact solutions from (1) and (5) are shown for comparison. The agreement is quite satisfactory.

Having verified the finite element approach, solution of various more complicated problems by finite elements is now feasible. These include rapid crack propagation in a statically loaded body and the wave interaction with a crack propagating either in a layered material parallel to layer interfaces (but not for a crack at the interface), or in a strip or halfspace parallel to its surface. Analysis of a crack moving in an orthotropic material is also possible, using the near tip fields as established numerically in Ref. [4]. Furthermore, extension to cracks propagating within the interface of two isotropic or orthotropic materials is possible, using the near tip fields determined in Refs. [6 and 7]. Geometric and some material nonlinearities in regions remote from the crack tip can also be included. It is also possible to solve cases in which the crack velocity changes discontinuously between time steps, while being constant within each time step; e.g. the case when a crack that is stricken by a wave remains at first stationary until a certain value of the stress intensity factor is reached, and then begins moving at a constant velocity  $c$ , thereby reducing the stress intensity factor.

However, application to bodies having finite dimensions in the direction of the crack is not possible without further extensions taking into account either the movement of the physical boundary through the grid or a deformation of the grid, by which the grid adapts itself to the fixed boundary. The latter extension has been explored to some extent, but the results have not been satisfactory thus far. Huge spurious oscillations have been obtained, which might have been due to the term  $\partial \rho / \partial x_1$ , on the right-hand side of eqn (20). Neglect of

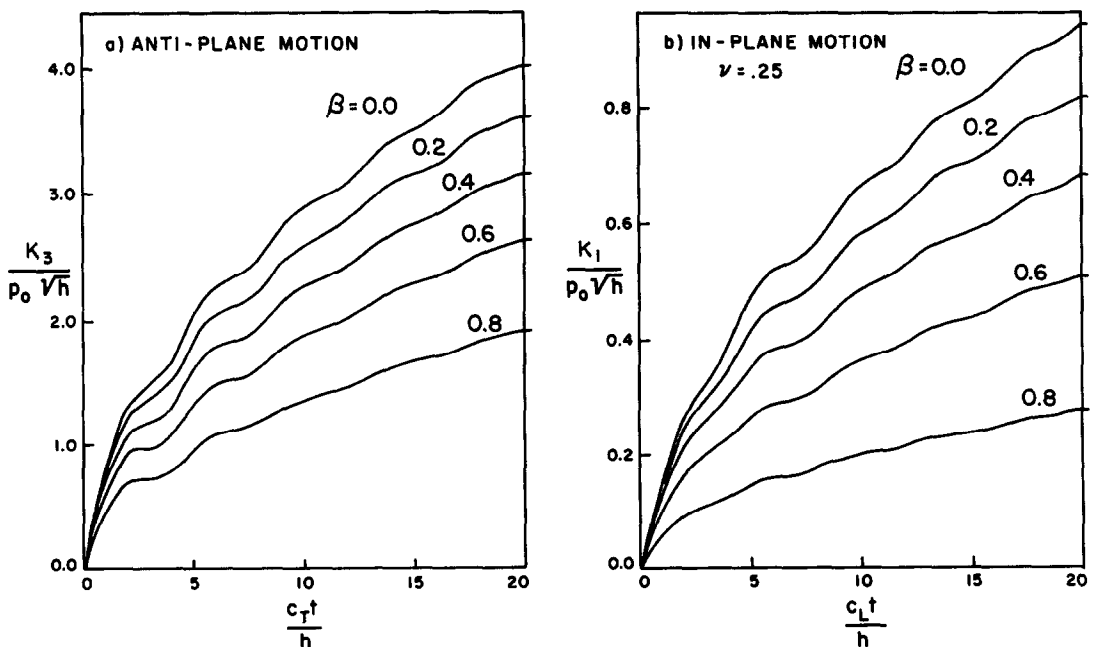


Fig. 2. Histories of the stress intensity factors  $K_3$  and  $K_1$  for various crack velocities  $c$ .

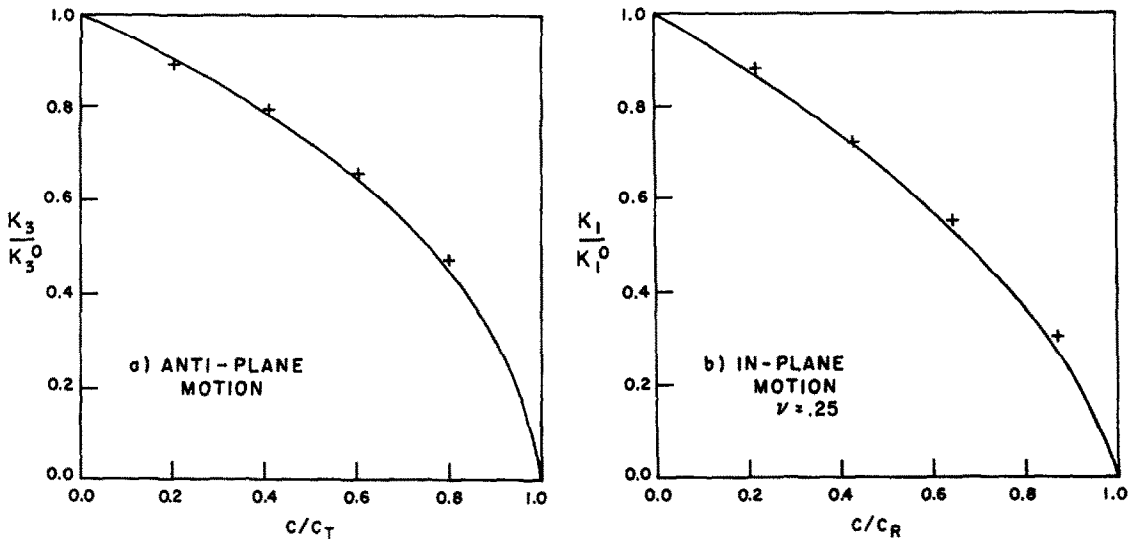


Fig. 3. Comparison of numerical values of  $K_3$  and  $K_1$  from Fig. 2 at final time  $T_1$  with the exact solutions [1, 5] for various crack velocities ( $K_3^0$  and  $K_1^0 =$  values of  $K_3$  and  $K_1$  at  $c = 0$  and  $t = T_1$ ,  $c_R =$  Rayleigh wave speed).

this term is inconsistent with the lumping of the mass which is necessary for other reasons[2].

#### CONCLUSIONS

1. The elastodynamic stress intensity factor due to the interaction of an elastic wave and a rapidly propagating crack can be solved with sufficient accuracy by the finite element method, if a grid which moves with the crack tip is used. In the present formulation only boundaries or material interfaces parallel to the crack can be accommodated.

2. The calibrated crack tip element method, in which the stress intensity factor is determined from its (statically calibrated) ratio to the crack opening displacement of a non-singular finite element at the crack tip, can be extended to dynamic problems with moving cracks. The dependence of the calibration ratio on crack velocity may be based on the near tip fields established before by analytical methods.

3. In case of a grid that moves rapidly through the solid, an additional apparent damping matrix results. This matrix is asymmetric which is unfavorable to the use of explicit time step integration algorithms. However, the iterative solution of the implicit time step equation system becomes very efficient in wave propagation problems, as they require a time step roughly equal to the travel time of a signal across the element, for which the contribution of the mass matrix makes the diagonal terms

of the equation matrix very large. An apparent additional stiffness matrix also results.

*Acknowledgement*—The work of two of the authors (J.D.A. and J.L.G.) was carried out in the course of research sponsored by the National Science Foundation under Grant ENG70-01465 A02.

#### REFERENCES

1. J. D. Achenbach, Dynamic effects in brittle fracture. In *Mechanics Today*. Vol. 1, pp. 1–57. (Edited by S. Nemat-Nasser) Pergamon Press, New York (1973).
2. Z. P. Bažant, J. L. Glazik and J. D. Achenbach, Finite element analysis of wave diffraction by a crack. *J. Engng Mech. Div. ASCE*, **102**, 479–496 (1976).
3. P. F. Walsh, Stress intensity factors by calibrated finite element method. Technical Note, *J. Engng Mech. Div. ASCE* **98**(EM6), 1611–1614 (1972).
4. J. D. Achenbach and Z. P. Bažant, Elastodynamic near-tip stress and displacement fields for rapidly propagating cracks in orthotropic materials. *J. Appl. Mech. Transactions Am. Soc. of Mech. Engrs.* **42**, 183–189 (1975).
5. B. R. Baker, Dynamic stresses created by a moving crack. *J. Appl. Mech. Transactions ASME*, **29** 449–458 (1962).
6. J. D. Achenbach, Z. P. Bažant and R. P. Khetan, Elastodynamic near-tip fields for rapidly propagating interface cracks. *Int. J. Engng Sci.* **16**, 797–809 (1976).
7. J. D. Achenbach, Z. P. Bažant and R. P. Khetan, Elastodynamic near-tip fields for a crack propagating along the interface of two orthotropic solids. *Int. J. Engng Sci.* **16**, 811–818 (1976).